

An innovative asphalt patch repair pre-heating method using dynamic heating

Juliana Byzyka^{*}, Mujib Rahman, Denis Albert Chamberlain

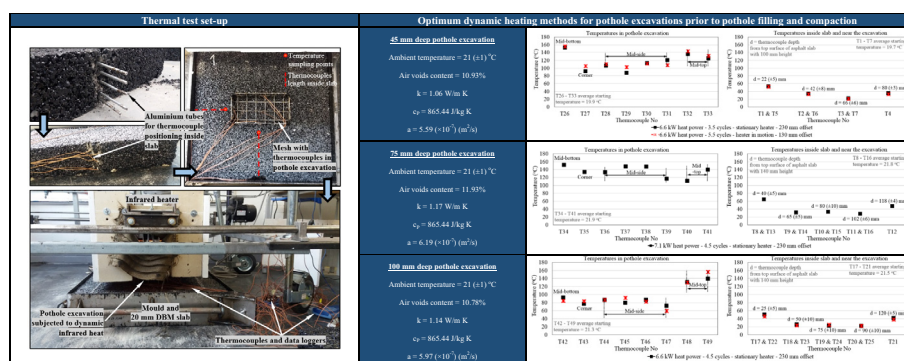
Department of Civil and Environmental Engineering, Brunel University London, Middlesex UB8 3PH, United Kingdom



HIGHLIGHTS

- Dynamic infrared heating aims to improve pothole repair interface bonding.
- Shallow and deep pothole excavations were subjected to dynamic infrared heating.
- Temperatures were measured on the excavation wall and inside the slab during heating.
- Temperatures in the excavations were significantly higher than inside the slab mixture.
- Temperatures inside the slab mixture had a lowering trend from the top to the bottom of the slab.

GRAPHICAL ABSTRACT



ARTICLE INFO

Article history:

Received 26 March 2018

Received in revised form 7 July 2018

Accepted 15 August 2018

Available online 23 August 2018

Keywords:

Asphalt
Pothole
Patch repair
Infrared heat
Dynamic heating

ABSTRACT

In hot mix asphalt patch repair, inadequate temperature at the interfaces is one of the influencing factors for inferior compaction and poor interface bonding. To enhance repair performance, a precisely controlled infrared pre-heating method for patch repair has been investigated. Asphalt slabs with 45 mm, 75 mm and 100 mm deep pothole excavations were subjected to dynamic heating with infrared heater operating power from 6.6 kW to 7.7 kW. The heater was kept either stationary or moving slowly across the excavations at 130 mm and 230 mm offsets. The tests included evaluating temperature increase throughout the excavations and inside the slab, recording heat power of infrared heater and heating time to avoid burning the asphalt. Irrespective of excavation depth, heating power and offset, the temperature distribution was found non-uniform in the pothole excavations and into the asphalt slab. The temperatures were higher at the faces of the excavation than inside the slab. Dynamic heating for approximately 10 min yielded better heat distribution while minimising the possibility of asphalt overheating and long pre-heating time. It has been concluded that 45 mm and 100 mm deep pothole excavations can be pre-heated with 6.6 kW and stationary heater or 7.5 kW and moving heater at 230 mm and 130 mm offset respectively. 75 mm deep excavation can be pre-heated with 7.1 kW and stationary heater at 230 mm offset.

© 2018 The Author(s). Published by Elsevier Ltd. This is an open access article under the CC BY license (<http://creativecommons.org/licenses/by/4.0/>).

^{*} Corresponding author.

E-mail addresses: juliana.byzyka@brunel.ac.uk (J. Byzyka), mujib.rahman@brunel.ac.uk (M. Rahman), denis@dac-consulting.co.uk (D.A. Chamberlain).

1. Introduction

1.1. Heating technology evolution in asphalt patch repair

One of the major distresses in asphalt pavement is potholes. They can be locally developed and are created due to the presence of water into the pavement and repeated traffic loading [1]. The main objective of permanently repairing a pothole is to create high quality repair in terms of (a) patching lifetime (this meaning quality and durability same as existing pavement), (b) low patching costs (high costs are mainly caused by labor, equipment and traffic control) [2], (c) minimum traffic disruption time ((b) and (c) can be achieved by fewer repetitions of the same patching), and (d) effective patching process (this referring to patching done in any weather conditions) [3]. To reach these objectives, infrared, microwave and induction heating has been used in asphalt paving operations for the last thirty to forty years.

Anderson and Thomas [4] mention that infrared or radiant heat is typically used for repairing overlays, smoothing and blending utility cuts and levelling of old patches. However, they do not recommend the use of infrared heat for full-depth repair. Blaha [3] built an automated patching machine and used infrared technology to heat asphalt to its softening point and ensure high bonding between the new fill mixture and old pavement. A comprehensive description of the machine is given, however, the procedure of the experiments and the study of heat flow to determine productive use of the heating system in asphalt repair are unclear and roughly explained. The study jumps to the conclusion of 1 min heating time for a surface asphalt softening point between 71 °C and 82 °C with the heater set to an extremely high heat power of 58 kW.

Clyne et al. [5], Uzarowski et al. [6], Freeman and Epps [7] and Leininger [8] used infrared or microwave heat to clear failed asphalt and/or heat the pothole fill material. The purpose of pre-heating was to achieve high adhesion between fill mixture and cold old pavement increasing its temperature. In these studies, only the surface temperature of the formed repairs is measured. The authors suggest a heating pattern and arrangement between the heater and distressed area to soften the asphalt. However, the authors do not acknowledge the influence of the following parameters in preheated asphalt repairs: climatic conditions, asphalt pavement temperature and thermal properties, asphalt ageing, repair geometry and pre-compaction temperatures of fill mixture. Further, the interaction between asphalt mixture and infrared heat has been studied mainly from on-site observations under diverse climatic conditions, not from controlled laboratory tests.

Obaidi et al. [9] performed, analysed and evaluated in the laboratory pothole repairs using asphalt tiles. They were bonded in the pothole cavity with a styrene-butadienestyrene (SBS) membrane filled with metal particles, steel fibres or chicken wire, induction heating and slight compaction. Tensile bond tests (TBT's) and shear bond tests (SBT's) were used to evaluate the tensile adhesion strength and shear strength respectively of the repair interface. The authors found that depending on the number of bonding layers, percentage of open area of loose fibres and induction heating time, maximum TBT and SBT were 0.35 MPa and 0.2 MPa respectively. In the case of the repairs with chicken wire of 37% to 74% open area, the TBT ranged from approximately 0.1 to 0.37 MPa and SBT ranged from 0.04 to 0.13 MPa.

Further, in the same study, test samples repaired with tiles and cold mix and test samples without any repair (original test samples) were tested using the wheel track test. The results showed that tests samples with asphalt tiles suffered 16.9% more rutting than the original test samples. Rutting in test samples with cold mix asphalt was approximately 40 times higher than in the original test samples. Therefore, tests samples with asphalt tiles outper-

formed repairs with cold mix. However, further research is suggested mainly when the excavated pothole contains loose stones or dirt between the tile and the old pavement or has uneven surfaces [9].

1.2. Infrared heat transfer in asphalt pavement

Thermal radiation is emitted by any object with a temperature above 0° Kelvin (−273 °C). Typical transmission of radiation is by electromagnetic waves that are defined by their wavelength and frequency categorized by the electromagnetic spectrum. The infrared portion of the spectrum is from 0.7 μm (equal to a 7e^{-7} m) to 10^3 μm (equal to a 1e^{-3} m). The energy transmitted by an infrared heater is proportional to its temperature. The higher the temperature, the shorter the wavelength and the higher the amount of energy radiated [10].

When the transmitted radiation energy of the heater hits the asphalt surface, then infrared heat transfer occurs. A portion of this radiation is absorbed and increases the temperature of the asphalt mixture by conduction, whereas other portions are transmitted or reflected back to the surrounding area [10]. Therefore, in an infrared-heater-asphalt thermal efficient relationship, the effectiveness of radiant energy emittance of the heater (associated with the heater emissivity (ε)), the transmitted percentage of radiative energy by the heater that strikes the asphalt (associated with the view factor (F)) and the amount of this energy absorbed by the asphalt (associated with asphalt emissivity (ε)) are dominant.

Other parameters to add to this relationship are the thermophysical properties of the asphalt mixture. These properties affect heat transfer and storage inside the pavement initiated by the absorbed radiation energy of radiative heat application on the surface of the pavement. There are two distinct categories of these properties: transport and thermodynamic properties. The transport properties relate to energy transfer through asphalt and are absorptivity (a), albedo ($1-a$), emissivity (ε) and thermal conductivity (k). The thermodynamic properties relate to the equilibrium state of asphalt mixture and are density (ρ) and specific heat capacity (c_p) [11].

Thermal conductivity of asphalt is affected by the mixture type, aggregate type [12], aggregate gradation [13], mixture density [14], mixture temperature [15] and presence of moisture in the mixture [13,14]. For example, Hassn et al. [14] found that as density increases thermal conductivity may increase too since the voids of air in the mixture decrease. In addition, moisture and freezing conditions may also increase asphalt thermal conductivity as reported by Mirzanimadi et al. [13]. However, asphalt thermal conductivity may decrease at temperatures higher than 25 °C reported by Chadbourn et al. [15]. Specific heat capacity and thermal diffusivity are both affected by thermal conductivity levels. For example, Hassn et al. [14] found that when air voids increase, and thermal conductivity decreases then specific heat capacity and thermal diffusivity decrease too.

1.3. Research motivation

As discussed above, heating the underlying layer prior to pothole filling and compaction enhances the bonding between the cold host pavement and the new hot-fill mix. Infrared, microwave and induction heating technologies have been investigated for this purpose. In the case of infrared heated repairs that concern this research, it seems that the current literature lacks fundamental experimental investigation and theoretical analysis of those repairs. To address this, the authors have concluded that the effect of the following parameters in the infrared repair operation should be investigated and fully understood: pothole geometry and depth; ambient temperature; host pavement initial temperature; fill mix-

ture temperature; host pavement and fill mixture thermophysical properties; infrared heater properties; infrared heating time; infrared heater offset and position; temperature distribution in host pavement external faces and heat flow inside the host pavement resulting from infrared heat application and repair work. This study has worked along these parameters to assess the use of infrared heat in asphalt repair and set a scientifically based foundation for infrared heated repairs. Below is described the status of each parameter set for this study:

- Pothole geometry: constant
- Pothole excavation depth: variable
- Host pavement thermophysical properties: investigated
- Fill mixture thermophysical properties: no fill mixture is included in this study
- Infrared heater properties: assumed constant (same infrared heater was used for all experiments but with different operating heat power)
- Infrared heating time: variable
- Infrared heater offset from host pavement surface: variable
- Infrared heater position: variable
- Temperature distribution in host pavement external faces: investigated
- Heat flow inside the host pavement: investigated

2. Experiments

2.1. Materials

Asphalt slabs were manufactured with 20 mm dense bitumen macadam (DBM). The mixture comprised of granite coarse and fine aggregate and limestone filler. The bitumen used was 100/150 pen. The mixture gradation curve is shown in Fig. 1 and its design con-

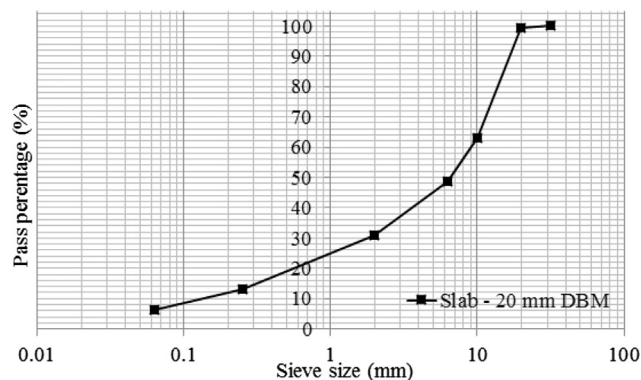


Fig. 1. Composition of slab asphalt mixture.

Table 1
Asphalt slabs construction parameters.

Slab no.	Mixture	Slab size: (L) × (W) × (H) mm ³	Pothole excavation size: (L) × (W) × (H) mm ³	Construction layers	Construction layers depth: mm
S1	20 mm DBM	695 × 695 × 100	305 × 165 × 45	2	50, 50
S2					
S3					
S4					
S5	20 mm DBM	695 × 695 × 140	305 × 165 × 75	3	50, 50, 40
S6					
S7					
S8					
S9	20 mm DBM	695 × 695 × 140	305 × 165 × 100	3	50, 50, 40
S10					
S11					
S12					

forms to BS EN 13108, part 1 (2016) [16]. The binder complies with the Manual of contract documents for Highway works, Volume 1, Specification for highway works (2008) [17]. The preparation of the aggregate, filler and bitumen prior to mixing, the asphalt mixing, and the control procedure of the mix temperature conform with BS EN 12697, part 35 (2016) [18].

2.2. Construction of asphalt slabs

The construction parameters of the asphalt slabs are shown in Table 1. The construction process for the 45 mm deep pothole excavations is shown in Fig. 2. For the 75 mm and 100 deep excavation similar construction method was followed but with a larger number of batches as shown in Table 1 and aluminium tubes (discussed in Section 2.3 below). In total twelve slabs of 695 (±5) mm × 695 (±5) mm were built. Each slab was designed with one pothole excavation of 305 (±2) mm × 165 (±2) mm located in the middle of it. The depths of the excavations were 45 (±2) mm, 75 (±2) mm and 100 (±2) mm with respective slab heights 100 (±5) mm and 140 (±5) mm. The chosen pothole depths represent shallow and deep potholes considering pothole depth range stated by the following authors. Miller and Bellinger [19] note that potholes may be deeper than 50 mm and McDaniel et al. [2] state that patches may range from 38 mm to 152 mm.

Each slab was constructed upside down in batches of 7.6 kg. Twelve, seventeen and eighteen asphalt batches were used to build slabs S1 – S4, S5 – S8 and S9 – S12 respectively. Slabs S1 – S4 were compacted in two lifts, whereas slabs S5 – S12 were compacted in three lifts. Each lift was approximately 50 mm deep and was compacted for 7 min using a vibrating plate as described in Standard Code of Practice, New Roads and Street Works Act 1991, Specification for the Reinstatement of Openings in Highways (2010) [20]. The lifts were bonded together by dynamically pre-heating each compacted lift with infrared heat to an average surface temperature 110 (±10) °C. The pre-heating time was 3 min.

The slabs were demoulded 19 h after their construction. The pothole moulds were removed using infrared heat. To do this, the heater was put above the pothole mould at 230 mm offset. The mould was then heated two or three times for 45 s with 1 min cooling time between the heating times. This was done to allow heat to be conducted from the pothole mould to the excavation wall and warm up the asphalt. The mould was then removed by manually pulling it out. There was not any destruction observed in the excavations with the conducted process.

2.3. Method for measuring temperatures within the pothole excavation under dynamic heating

T-type thermocouples (accuracy of 0.5 °C) [21] were used to measure real-time temperatures inside the slabs under dynamic



Fig. 2. Slab construction with embedded aluminium tubes to accommodate thermocouples for thermal tests: (a) moulds set up; (b) and (c) 4 aluminium tubes between six asphalt batches of first lift; (d) compacted first lift; (e) pre-heating of compacted lift; (f) and (g) 3 aluminium tubes between six batches of second lift; (h) compacted second lift; (i) slab turned upside down and pothole mould removed after 19 h of construction; (j) slab section A-A'.

infrared heating. The positions of the thermocouples are described in [Tables 2 and 3](#) and shown in [Fig. 3](#). Hollow aluminium tubes, 4 mm in diameter, were put into the slabs during their construction to accommodate the thermocouples. For a 45 mm deep pothole excavation, 4 slabs (S1–S4, [Table 2](#)) were in total built and 7 aluminium tubes of lengths L1, L2 and L3 ([Table 3](#)) were put at varying depths inside each slab. Six tubes were fixed perpendicular to sides 1 and 2 shown in [Fig. 2\(b\)](#), (c) and (f) and one tube was

positioned below and near the bottom face of the excavation ([Fig. 2\(g\)](#)). Although the positioning of the tubes for all slabs was similarly done, the tubes moved during the construction of the slabs. This is expected to have been mainly happening during the compaction of the slab mixture. For example, [Tables 2 and 3](#) show that thermocouple T1 measured temperature in a depth from the slab surface of 22 (± 5) mm and a distance L2 = 243 (± 5) mm ([Fig. 3](#)). This means that temperature at T1 may have been mea-

Table 2

Position of thermocouples laying inside the slabs.

Slab no.	Slab depth: mm	Pothole excavation type	Thermocouple (T) no.		Depth (d): mm
			Side 1	Side 2	
S1 – S4	100	45 mm deep	T1	T5	22 (±5)
			T2	T6	42 (±8)
			T3	T7	66 (±6)
			T4	–	80 (±3)
S5 – S8	140	75 mm deep	T8	T13	40 (±5)
			T9	T14	65 (±5)
			T10	T15	80 (±10)
			T11	T16	102 (±6)
			T12	–	118 (±4)
			T17	T22	25 (±5)
S9 – S12	140	100 mm deep	T18	T23	50 (±10)
			T19	T24	75 (±10)
			T20	T25	90 (±10)
			T21	–	120 (±5)

Table 3

Length of thermocouples laying inside the slabs.

Lengths: mm								
L1	L2	L3	L4	L5	L6	L7	L8	L9
165 (±13)	243 (±5)	355 (±1)	165 (±15)	243 (±15)	360 (±10)	165 (±15)	243 (±150)	360 (±5)

sured in a depth of 17 mm–27 mm and at a distance of 238 mm–248 mm. Similarly, but nine aluminium tubes in number, were set inside the slabs for the 75 and 100 mm deep excavations.

T-type thermocouples [21] were also used to measure temperatures at eight points into the pothole excavations. A thin steel mesh was used to keep the thermocouples in place during the application of dynamic heat. The mesh helped also to retain the shape of the excavations. Two thermocouples were placed at the bottom corner and mid-area respectively of the excavation, four thermocouples were placed in the middle of the excavation vertical sides, and two thermocouples in the mid-top periphery of the excavation (Fig. 4 and Table 4).

2.4. Description of infrared heating equipment and dynamic heating method for thermal tests

The parameters of the thermal tests are summarised in Table 5. An experimental infrared heater was used to perform the thermal tests of this study. The heater is described in Byzyka et al. [22] and is shown in Fig. 5 of Section 2.5. The heater consists of a steel frame of 1.60 m (L) × 1.55 m (W). The frame has adjustable height and is supported by four wheels. The heater contains two heating elements of 165 mm (L) × 455 mm (W) × 102 mm (H). They can operate at heat powers between 6.6 kW and 7.7 kW and they can be set to be either stationary or moving over the pavement with a constant speed of 0.04 m/s. The heater is operated by its central control unit.

For the thermal tests, the pothole excavations were heated in heating–cooling cycles, referred to as “dynamic heating”. For the heating part of the cycle, the heater was operating at heat powers 6.6 kW, 6.7 kW, 7.1 kW, 7.5 kW and 7.7 kW. The excavations were heated until the thermocouples closest to the heating element plate (see T32, T33, T40, T41, T48 and T49 in Fig. 4 and Table 4) measured asphalt temperatures between 140 °C and 160 °C. This was done to avoid burning the asphalt. Similar asphalt heating levels are also suggested by previous studies. Uzarowski et al. [6] suggest heating the repair area to a temperature not greater than 190 °C. Nazzal et al. [23] suggest to pre-heat the old pavement until temperatures reach 135 °C to 190 °C levels. In addition, Huang et al. [24] note that heating asphalt between 137 °C and

226 °C reduces ageing or charring of asphalt binder. Asphalt ageing happens due to volatilisation, oxidation, and other chemical processes. Asphalt oxidation should be avoided because it leads to pavement failure due to asphalt binder hardening, change in viscosity, asphalt separation, asphalt embrittlement, loss of bitumen cohesion and bitumen-aggregate adhesion [25]. For the cooling part of the cycle, the heater was simply turned off and no heating was applied until temperatures of T32, T33, T40, T41, T48 and T49 reached temperatures between 70 °C and 80 °C. This was done to allow heat to be conducted within the slab and warm up the asphalt mixture around the pothole excavations.

Further, the tests were conducted with heating applied at 130 mm and 230 mm offsets from the surface of the slab. The heating elements were stationary above the excavations or moving across the excavations. The moving distance within the heater steel frame was 1 m. This distance could be automatically set to be covered by the heating elements by moving forward and backwards repetitively within heater steel frame.

2.5. Thermal tests set up

Dynamically heating the pothole excavation is intended to improve common pothole repair practices with or without pre-heating to ultimately increase interface bonding and therefore pothole repair durability. The pothole pre-heating method studied in this paper would be expected to follow after the failed asphalt mixture of the pavement is removed and the excavation is cleaned from debris and water. Since the pothole excavations studied in the paper were artificially created, these steps were not included in the described processes.

The thermal test set up is shown in Fig. 5. Sixty thermal tests were in total completed (20 tests per pothole excavation depth). Temperatures were measured for a dynamic heating duration of approximately 30 min. The tests were performed 30 days after the construction of the slabs and measurement of thermal conductivity. As the sample size was big, this timeframe was necessary to optimise laboratory resources during sample preparation and production and carry out additional test (like thermal conductivity) on the whole sample. The ambient temperature during the tests ranged between 20 °C and 22 °C.

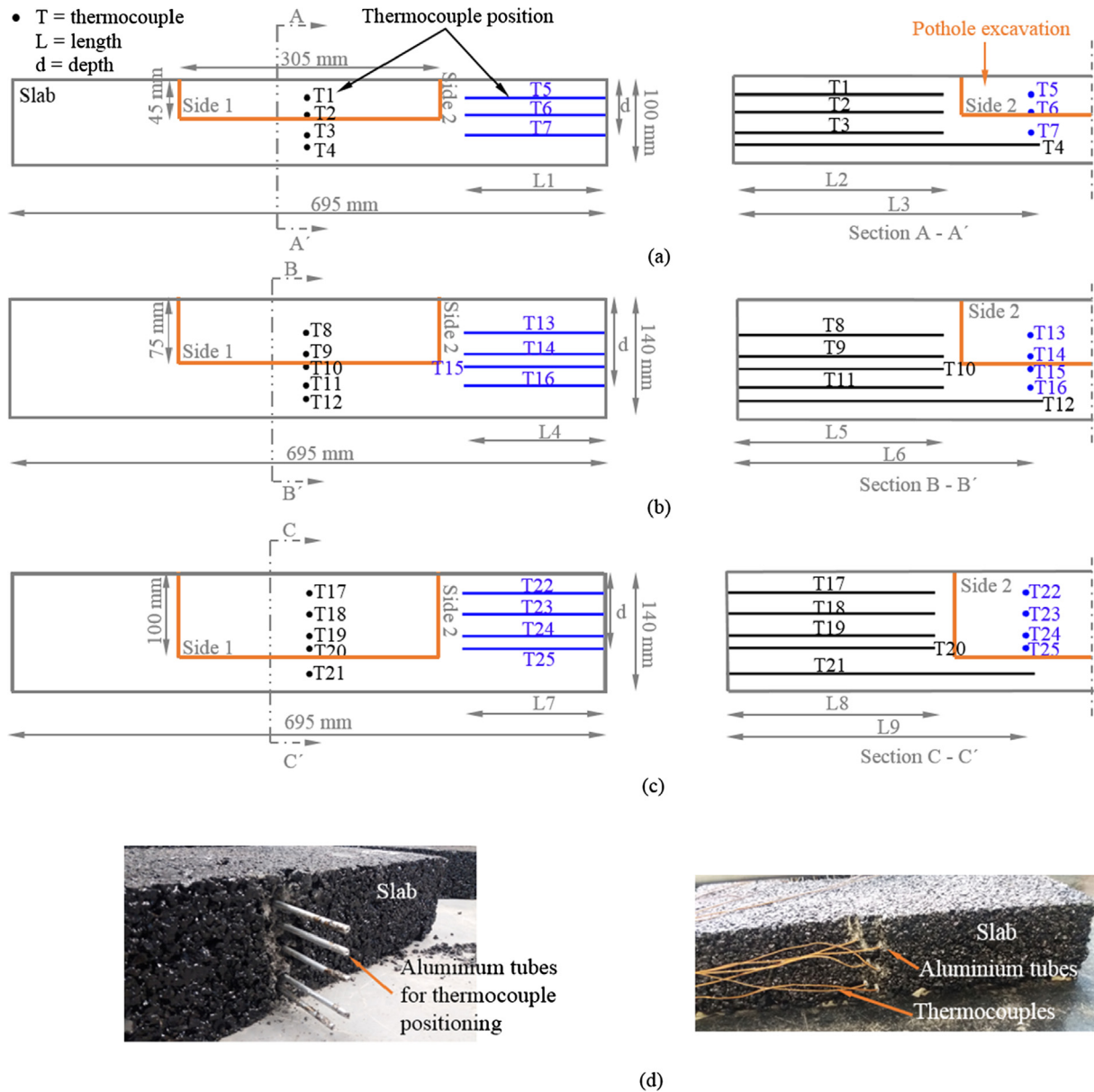


Fig. 3. Demonstration of thermocouple positions and lengths laying inside the slabs for (a) 45 mm; (b) 75 mm; and (c) 100 mm deep pothole excavations. The physical implementation of the previous sketches is shown in (d).

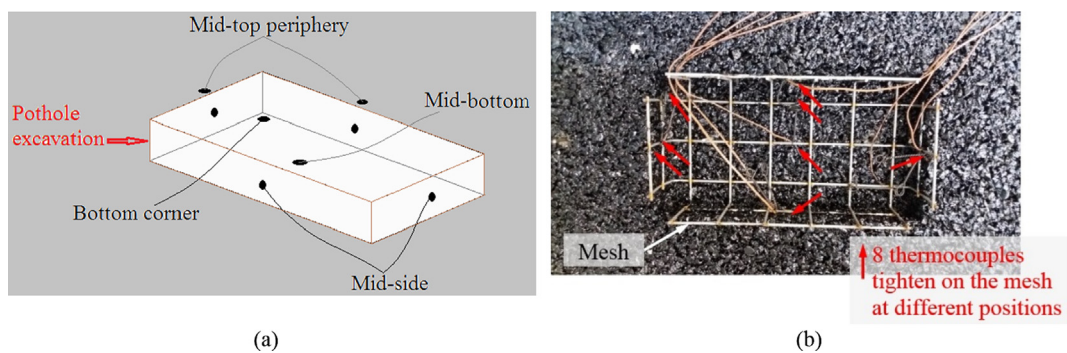


Fig. 4. Thermocouples in the pothole excavation: (a) sketch; (b) physical implementation.

Table 4

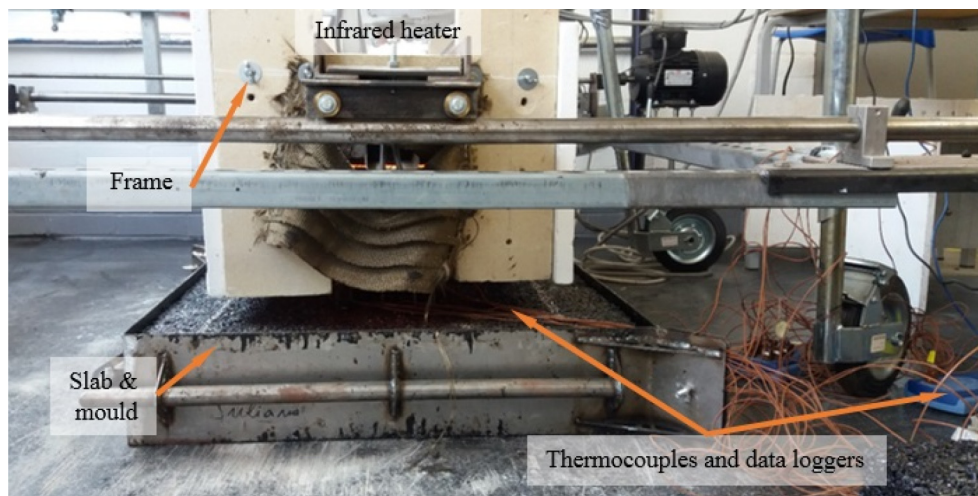
Characterisation of thermocouples in the pothole excavation

Slab no.	Pothole depth	Thermocouple positions							
		Mid-bottom	Bottom-corner	Mid-side				Mid-top	
S1 – S4	45 mm	T26	T27	T28	T29	T30	T31	T32	T33
S5 – S8	75 mm	T34	T35	T36	T37	T38	T39	T40	T41
S9 – S12	100 mm	T42	T43	T44	T45	T46	T47	T48	T49

Table 5

Thermal test parameters

Slab no.	Heat Power: kW	Heater offset from slab top surface: 130 mm		Heater offset from slab top surface: 230 mm	
		Stationary heater	Moving heater	Stationary heater	Moving heater
S1	6.6, 6.7, 7.1, 7.5 and 7.7	✓			
S2			✓		
S3				✓	
S4					✓
S5	6.6, 6.7, 7.1, 7.5 and 7.7	✓			
S6			✓		
S7				✓	
S8					✓
S9	6.6, 6.7, 7.1, 7.5 and 7.7	✓			
S10			✓		
S11				✓	
S12					✓

**Fig. 5.** Thermal test setup for stationary and moving heater.

3. Asphalt thermal properties

3.1. Thermal conductivity (k)

For this study, thermal conductivity was measured at eleven points per slab prior to commencing the thermal tests. During the measurement of thermal conductivity, the ambient temperature ranged between 18.5 °C and 22.5 °C. At the same time, the temperature of the slabs ranged between 20.5 °C and 22 °C. Thermal conductivity was measured with the transient line source (TLS) [26] shown in Fig. 6. The temperature of the slabs was also measured using the TLS.

The TLS includes the TLS controller and a 50 mm needle designed for testing samples that are tough to drill such as rock, concrete or asphalt samples. The TLS has an accuracy of 5% and reproducibility of 2%. The TLS method follows ASTM D5334 (2000) [27] and has been previously used in investigations of thermal conductivity by Chadbourn et al. [15], Blázquez et al. [28] and Lu et al. [29]. To measure thermal conductivity with the TLS-50

first a 4 mm (D) x 50 mm (H) hole was drilled in the asphalt slab. Then, the excess powder in the hole from drilling was blown out with compressed air. The needle was covered with a thermal paste called Arctic Alumina [30] before inserting it completely into the slab. The thermal paste helps to fill any air gaps in the hole and promote good thermal contact between the slab mixture and the needle. Thermal conductivity was calculated by the TLS using Eq. (1):

$$k = \frac{q}{4\pi a} \quad (1)$$

where k = thermal conductivity, W/m K; q = heating power, W; a = slope. The slope comes from a plot of temperature rise in the sample when heated by the TLS versus the logarithm of time [26].

3.2. Specific heat capacity (c_p) and thermal diffusivity (a)

Specific heat capacity (c_p) and thermal diffusivity (a) were calculated using Eq. (2) [14] and Eq. (3) [15] respectively:

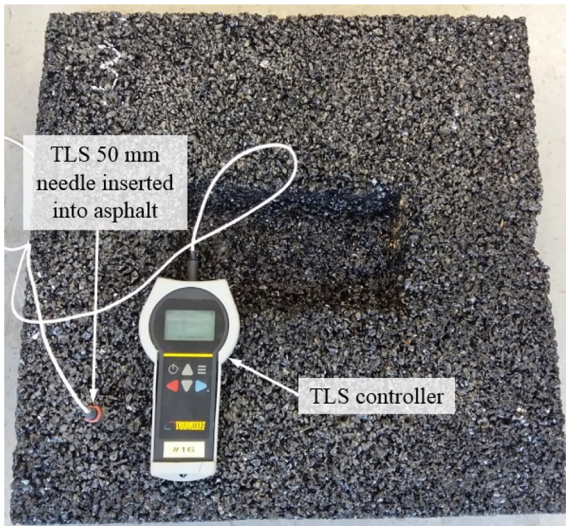


Fig. 6. TLS-50 instrument for measurement of asphalt thermal conductivity.

$$C_p = \frac{1}{m_{\text{total}}} [m_{\text{aggregate}} \times C_{\text{aggregate}} + m_{\text{bitumen}} \times C_{\text{bitumen}}] \quad (2)$$

where m = mass of each material, kg; and c = specific heat capacity of each material, J/kg K.

$$a = \frac{k}{\rho c_p} \quad (3)$$

where ρ = density, kg/m³.

4. Air voids content

The air voids content of the compacted asphalt slabs was calculated based on the calculation of the maximum specific gravity and the maximum theoretical specific gravity of asphalt mixture. The bulk specific gravity (G_{mb}) was determined through the AASHTO T166 (2007), method A [31] and the maximum theoretical specific gravity (G_{mm}) was calculated with Eq. (4) [32]. In this equation, the effective specific gravity of aggregate (G_{se}) was used as 2.65 and the specific gravity of bitumen (G_b) as 1.01. Thereafter, the percentage of air voids in the mixture was calculated with Eq. (5).

$$G_{mm} = \frac{W_T}{\frac{W_{agg}}{G_{se}} + \frac{W_{AC}}{G_b}} \quad (4)$$

where W_T = total weight of asphalt mixture, gr; W_{agg} = weight of aggregate, gr; W_{AC} = weight of total asphalt binder, gr.

$$VTM = \left(1 - \frac{G_{mb}}{G_{mm}}\right) \times 100\% \quad (5)$$

where VTM = voids in total mix, %.

5. Results and discussion

5.1. Thermophysical properties

Table 6 shows air voids, thermal conductivity, calculated specific heat capacity and thermal diffusivity of the compacted asphalt slabs. The table shows the percentage of air voids from the average of five cores per slab for slabs S1 and S2 and from the average of eight cores per slab for slabs S3 to S12. The cores were extracted throughout the whole sample in order to test overall air voids distribution.

The cores were extracted from the slabs at the end of the thermal tests conducted per slab. After the coring, the slabs were not used in any testing. The results show that air voids content ranged from 10% to 13%. The effect of asphalt preheating in air voids has not been investigated in this study due to lack of laboratory equipment and no other study for infrared heated patch repair was found to mention it. However, the authors acknowledge that in some areas of the slabs, air voids may have been reduced, while in other areas they may have been increased. This assumption was done after Norambuena-Contreras and Garcia [33] noted similar effect of microwave and induction heating in asphalt mixture air voids. The affected areas by the pre-heating would probably be those closer to the heated pothole excavation, near the heater where some cores were also taken or in the areas where heat was conducted due to excavation pre-heating.

Table 6 demonstrates that thermal conductivity of the asphalt slabs ranged from 0.98 W/m K to 1.24 W/m K. The results show that thermal conductivity is significantly affected by the high percentage of air voids in the slabs. This happened because air has much lower thermal conductivity (0.025 W/m K [34]) compared to the thermal conductivity of granite aggregate (2.68 W/m K [34]) and limestone filler (2.92 W/m K [35]) used in this study and binder (0.39 W/m K [36]). High air voids mean also lower interlocking between the aggregates of the mixture, less thermal conductance paths into the asphalt mixture and therefore lower thermal conductivity. This effect of air voids in asphalt thermal conductivity has been also reported by Mirzanamadi et al. [13] and Hassn et al. [14].

Further, in this study, thermal conductivity was measured with the TLS method. The TLS needle was inserted into holes drilled throughout the slabs and thermal conductivity was calculated by the TLS controller using the heat conduction equation. This means

Table 6
Thermophysical properties of asphalt mixture

Slab no.	Core diameter (mm)	Core height	Air voids content (%)	Thermal conductivity (W/m K)	Specific heat capacity (J/kg K)	Thermal diffusivity ($\times 10^{-7}$) (m ² /s)
1	72	1 core of 55 mm & 4 cores	10.04%	1.12	865.44	5.84
2	72	of 100 mm per slab	10.51%	1.05	865.44	5.52
3	72		11.99%	0.98	865.44	5.20
4	72		11.18%	1.10	865.44	5.78
5	72	2 cores of 65 mm & 7 cores	13.08%	1.24	865.44	6.72
6	72	of 140 mm per slab	11.52%	1.11	865.44	5.86
7	72		12.25%	1.09	865.44	5.80
8	72		10.88%	1.22	865.44	6.39
9	72	2 cores of 40 mm & 7 cores	10.74%	1.00	865.44	5.26
10	72	of 140 mm per slab	10.79%	1.16	865.44	6.08
11	72		11.10%	1.18	865.44	6.18
12	72		10.47%	1.22	865.44	6.36

that the measurement of thermal conductivity was affected by the distribution of mineral materials around the drilled hole, the cleanliness of the hole and the thermal contact between the asphalt mixture and the needle.

In addition, specific heat capacity was found equal to 865.44 J/kg K. Specific heat capacity is considerably affected by the temperature and mass of the asphalt mixture. In this study, both parameters remained at similar levels for all slabs. Finally, thermal diffusivity had been found to range between $5.20 \times 10^{-7} \text{ m}^2/\text{s}$ and $6.72 \times 10^{-7} \text{ m}^2/\text{s}$. These values were affected by the range of the thermal conductivity and volumetric heat capacity. The discussed effect is also noted by Mirzanamadi et al. [13] and Hassn et al. [14].

5.2. Temperature distribution under dynamic heating

The temperatures captured in the 45 mm, 75 mm and 100 mm deep excavations wall and inside the slabs are presented in Figs. 7–12. Figs. 7, 9 and 11 show temperature profiles for stationary heater above the excavations. Whereas, Figs. 8, 10 and 12 show temperature profiles for moving heater across the excavation. Each figure contains ten graphs and demonstrates temperatures per thermocouple position at the end of approximately 10 min, 20 min and 30 min dynamic heating. Temperatures are reported for operation of heater with 6.6 kW, 6.7 kW, 7.1 kW, 7.5 kW and 7.7 kW heat powers and for 130 mm and 230 mm heater offsets. The slab number used to perform the thermal tests and the number of heating-cooling cycles for each dynamic heating time are also reported. All thermal tests finish with the heating part of the cycles (or half cycle) and therefore the heating-cooling cycles are reported with numbers such as 3.5, 6.5, 8.5 etc. For example, in Fig. 7, for 10 min dynamic heating and heater operating at 6.6 kW heat power at 130 mm offset, three and a half cycles were done. For the three whole cycles, the heater was on and off repeatedly. For the half-cycle, the heater was on for some time and then removed from the pothole pre-heating procedure. The heating-cooling cycle procedure was also described in Section 2.4.

Overall, the results show higher temperatures in the faces of the pothole excavation than inside the slabs. This happened because the temperatures in the excavation increase due to radiation. Whereas, the percentage of the heater radiative energy that reaches the slab and is absorbed by it will increase the temperature of the asphalt mixture inside the slab. The absorptivity of asphalt mixture depends on the colour of the mixture, as light colour asphalt surfaces have higher reflectance [37], and the surface roughness [38]. Hassn et al. [14] showed that asphalt pavements with high percentage of air voids, like the slabs in this study, have higher reflectance than pavements with lower percentage of air voids. This happens because the illumination surfaces and angles are higher for high air void content mixtures [38]. Once the heater energy is absorbed by the asphalt, the increase of mixture temperature inside the slabs depends on initial slab temperature and heat transfer mainly due to conduction which is dependent on the thermal properties of the mixture.

5.2.1. Slabs with 45 mm deep pothole excavation

The heating effects of dynamic heating are shown in Figs. 7 and 8. It is observed that temperatures in the pothole excavation and inside the slab were increased non-uniformly. The temperature increase rate inside the slab was higher for the first 10 min of heating than between 10 min and 30 min of heating. This happened because thermal conductivity decreases while mixture temperature increases. The effect of temperature in thermal conductivity of asphalt mixture was not measured in this study. However, it has been previously noted by Chadbourn et al. [15] for

temperatures between 25 °C and 75 °C and by Pan et al. [35] for temperatures between –20 °C and 60 °C. Further, Pan et al. [35] suggest that the decrease of thermal conductivity at higher mixture temperatures is mainly affected by the thermal conductivity of aggregates, as they account for more than 90% of the mixture, than the thermal conductivity of the binder.

Overall, temperatures measured in the mid-bottom of the pothole excavation (T26) exhibited the highest increase in temperature and reached 140 °C to 160 °C. High temperatures but lower than T26, mainly in the region of 120 °C to 140 °C, were observed in the mid-top periphery of the pothole excavation (T32 and T33). There were two reasons that T26 had higher temperatures than T32 and T33. Firstly, temperatures on the heating element plate were higher in the central region of the plate than in the periphery and the ends of the plate (this is shown in Ref. [22]). Secondly, T32 and T33 were located at the top of the excavation periphery and it seems that the heat loss was higher in those points than at the bottom of the excavation. This also shows that the effect of the external environment was higher for T32 and T33 than T26. In addition, the lowest temperatures were observed in the sides (T28–T31) and the corner (T27) of the pothole excavation. This shows that the heater had a larger view of the points located in the horizontal faces of the pothole excavation than the points located in the vertical faces of the excavation. To this extent, temperatures for T28–T31 and T27 ranged from 80 °C to 120 °C.

Overall, temperatures in the pothole excavation were higher for 7.7 kW than for 6.6 kW. However, no increasing or decreasing trend was observed for temperatures resulted for heater heat powers in between the 6.6 kW–7.7 kW range. This meaning that temperatures in the pothole excavation may either increase or decrease without depending on the heater heat power between the noted above heat power range. Similar reaction was also observed when excavation temperatures were compared (a) between 130 mm and 230 mm heater offsets for stationary and moving heater for each heater operating heat power and (b) between stationary and moving heater for 130 mm and 230 mm heater offsets for each heater operating heat power.

Heat inside the slabs was transferred from top to bottom. Temperatures tend to increase during the heating-cooling cycles but had a lowering trend from the top to the bottom of the slabs. The latter is mainly attributed to the slow heat transfer due to low thermal conductivity and volumetric specific heat capacity of the asphalt mixture of this study. Overall, thermocouples T1 and T5 located closer to the top surface of the slabs captured temperatures between 40 °C and 80 °C. Below T1 and T5, temperatures for T2–T4, T6 and T7 ranged from 20 °C to 70 °C. A similar pattern in temperature increase between temperatures in pothole excavation and inside the slabs was observed for the three different durations of dynamic heating with heater being either stationary or in motion.

5.2.2. Slabs with 75 mm deep pothole excavation

The temperature profile under dynamic heating is shown in Figs. 9 and 10. Similarly, with the 45 mm deep pothole excavation, temperatures inside the slab were lower than in the excavations as a result of the thermal properties of the mixture. Temperatures inside the slabs showed also a lowering trend from top to bottom. The effect of dynamic heating in the temperatures of the excavation faces was larger for 230 mm heater offset than 130 mm offset. This happened for all heat powers with stationary heater above the excavation and for heat powers between 6.7 kW and 7.5 kW for moving heater. However, temperature was at similar levels in the pothole excavation for moving heater with 6.6 kW and 7.7 kW and 230 mm heater offset. Overall temperature distribution in the 75 mm deep pothole excavation was more uniform than in

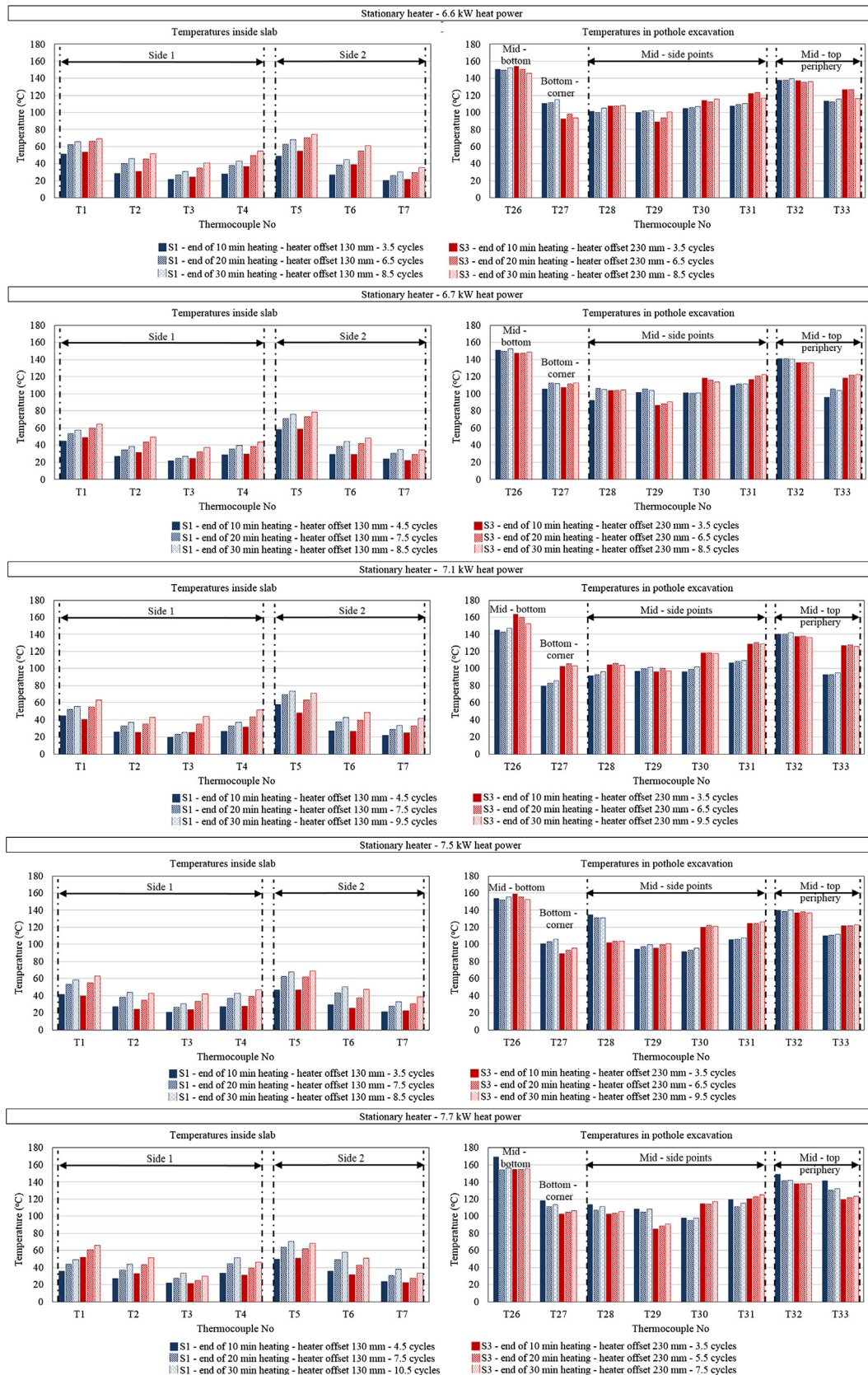


Fig. 7. Temperature distribution in 45 mm deep pothole excavation and stationary heater.

the 45 mm deep pothole excavation for stationary heater. T39 located in one of the vertical faces of the excavation was the only thermocouple that had lower temperatures than the rest of the

excavation. This may have happened because the thermocouple moved or was mistakenly covered by a wire of the steel mesh that was holding the thermocouples in place during the thermal tests.

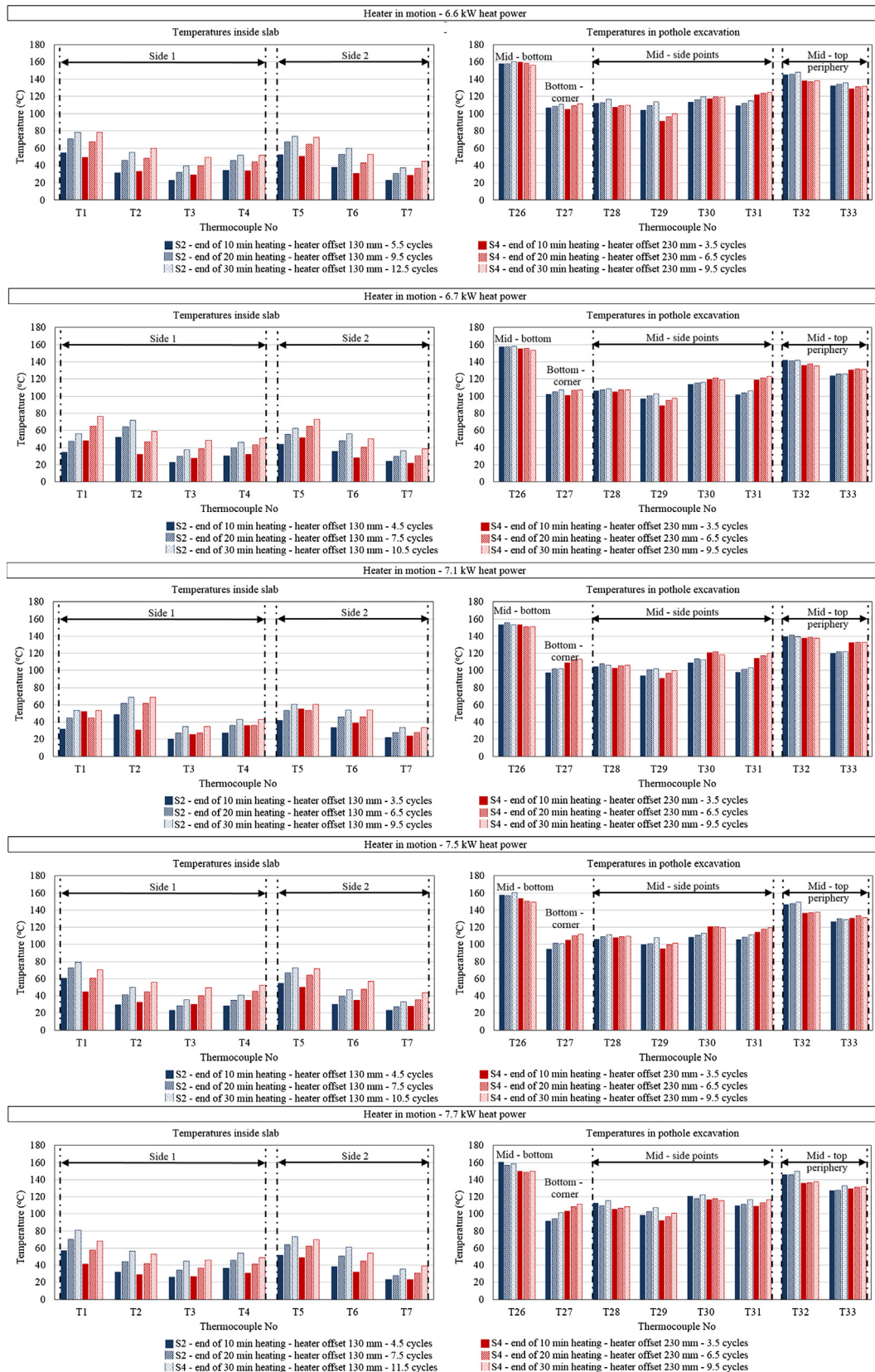


Fig. 8. Temperature distribution in 45 mm deep pothole excavation and moving heater.

From Fig. 10, it is also observed that for moving heater thermocouple T41 had significantly lower temperatures than T40 although both thermocouples were located at the top of the exca-

vation. This happened because the heater was moving across the excavation and perpendicular to the long sides of the pothole where T41 was located in the middle of it. The air circulation

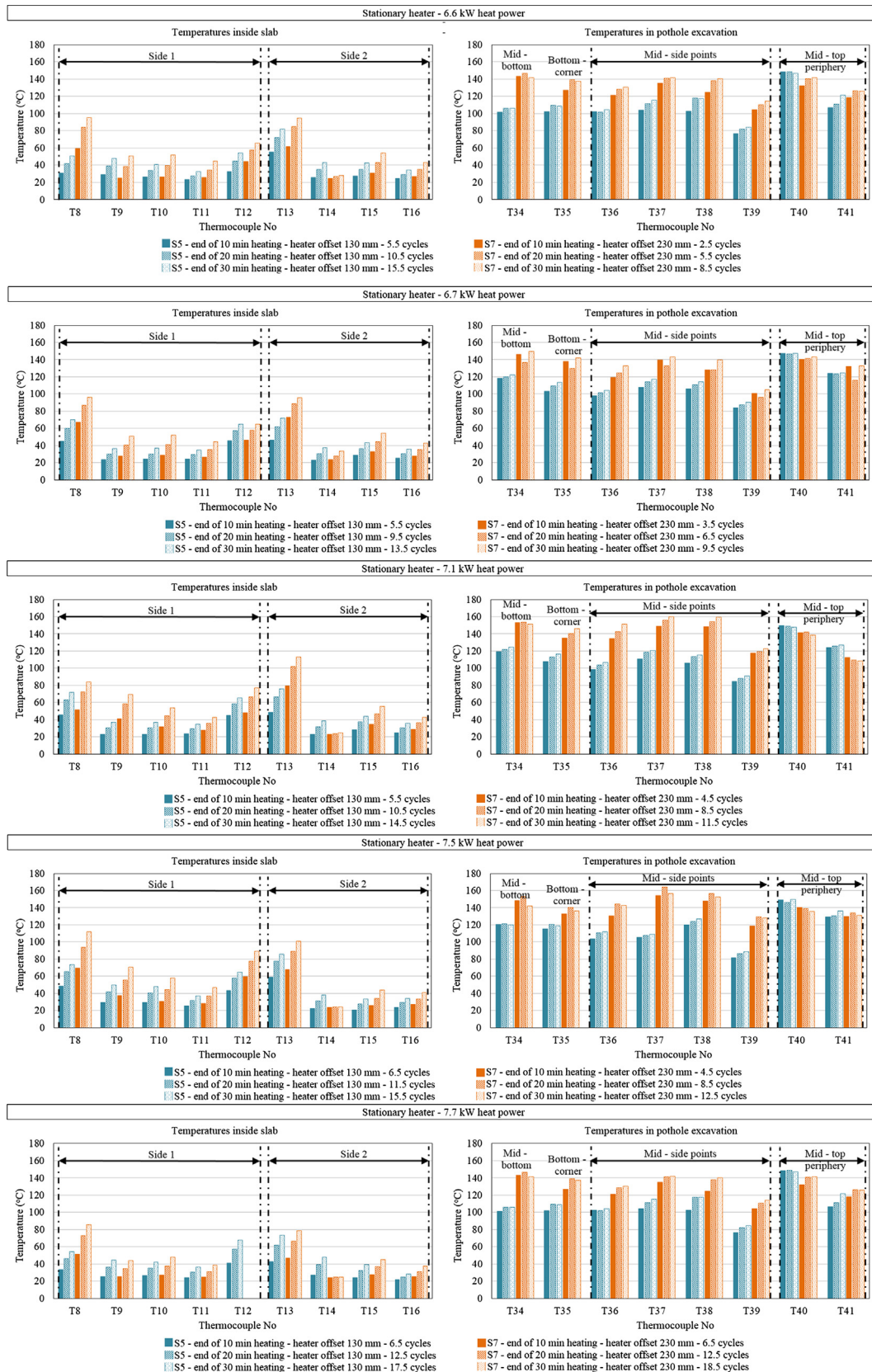


Fig. 9. Temperature distribution in 75 mm deep pothole excavation and stationary heater.

due to the moving heater seems to have significantly affected and cooled down the temperatures of T41 compared to T40.

Reflecting the above, between 10 min and 30 min heating for stationary heater at 130 mm offset, temperatures for T34–T38 were

94 °C – 130 °C; for T39 were 76 °C – 91 °C; for T40 were 143 °C – 150 °C; and for T41 were 106 °C – 136 °C. Whereas, at heater offset 230 mm, temperatures for T34–T38 were 103 °C – 164 °C; for T39 were 89 °C – 129 °C; for T40 were 135 °C – 146 °C; and for T41 were

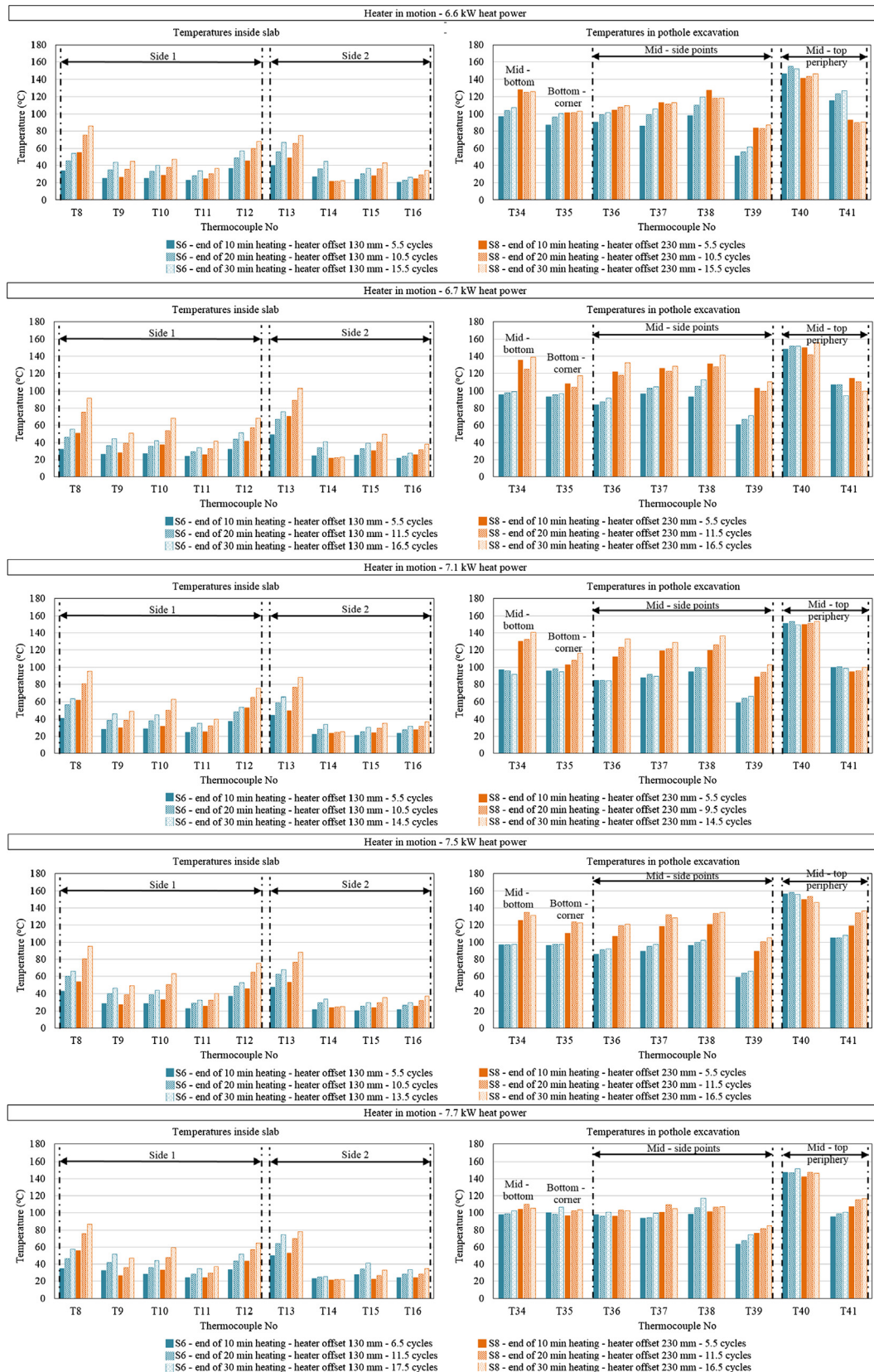


Fig. 10. Temperature distribution in 75 mm deep pothole excavation and moving heater.

90 °C – 134 °C (Fig. 9). For moving heater at 130 mm offset temperatures for T34-T38 were 84 °C – 117 °C; for T39 were 51 °C – 74 °C; for T40 were 146 °C – 158 °C; and for T41 were 94 °C – 127 °C.

Whereas, at heater offset 230 mm, temperatures for T34-T38 were 96 °C – 140 °C; for T39 were 83 °C – 110 °C; for T40 were 140 °C – 156 °C; and for T41 were 90 °C – 137 °C (Fig. 10).

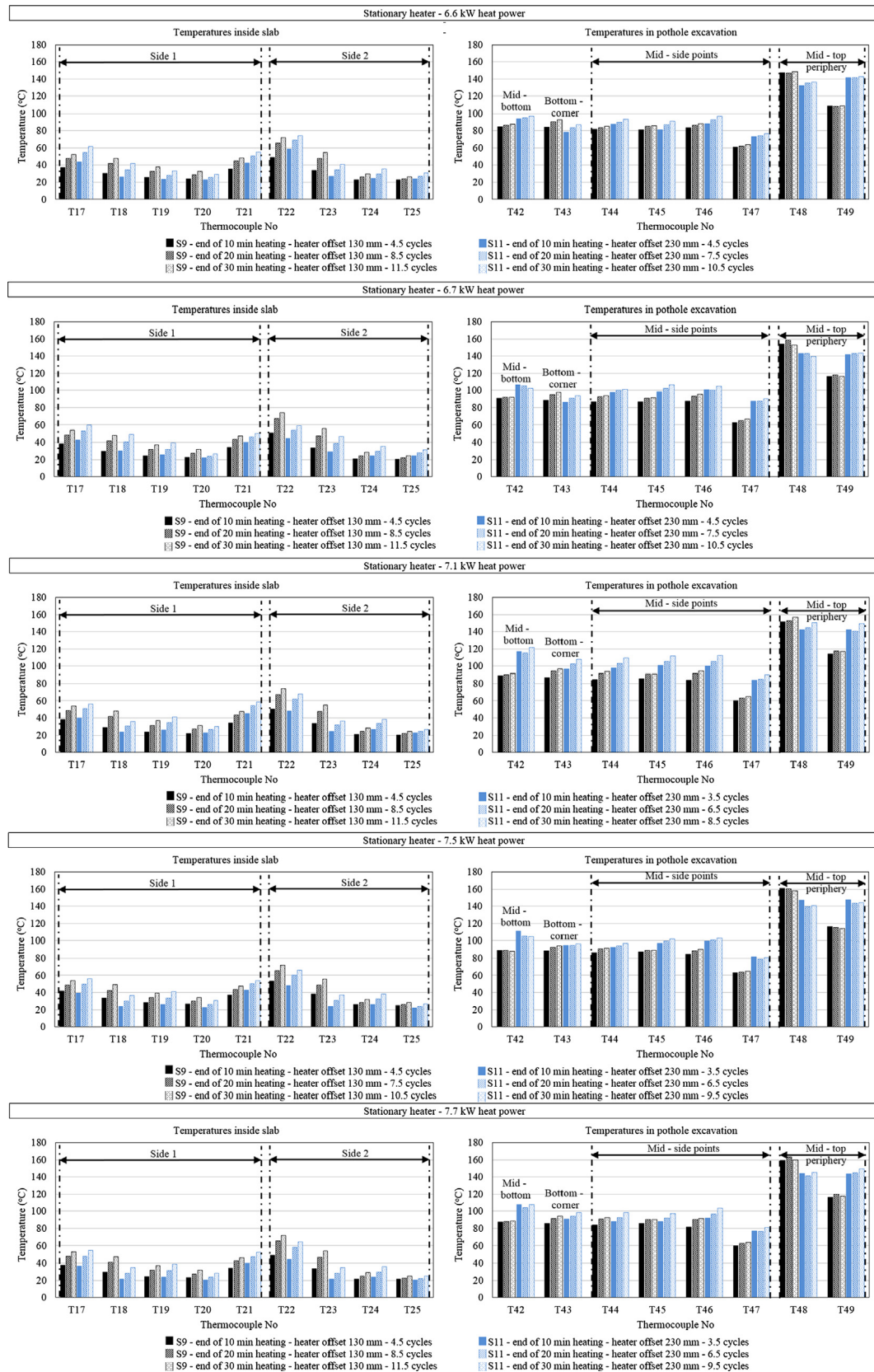


Fig. 11. Temperature distribution in 100 mm deep pothole excavation and stationary heater.

For internal slab temperatures, for both stationary and heater in motion at 130 mm offset, temperatures were fluctuating from 30 °C to 70 °C for T8. This sensor was located closer to the top surface of the

slab. Below T8, temperatures ranged between 25 °C and 50 °C (T9–T11 and T14–T16). Similar temperatures to T8 were captured from thermocouple T12 located below the bottom surface of the pothole

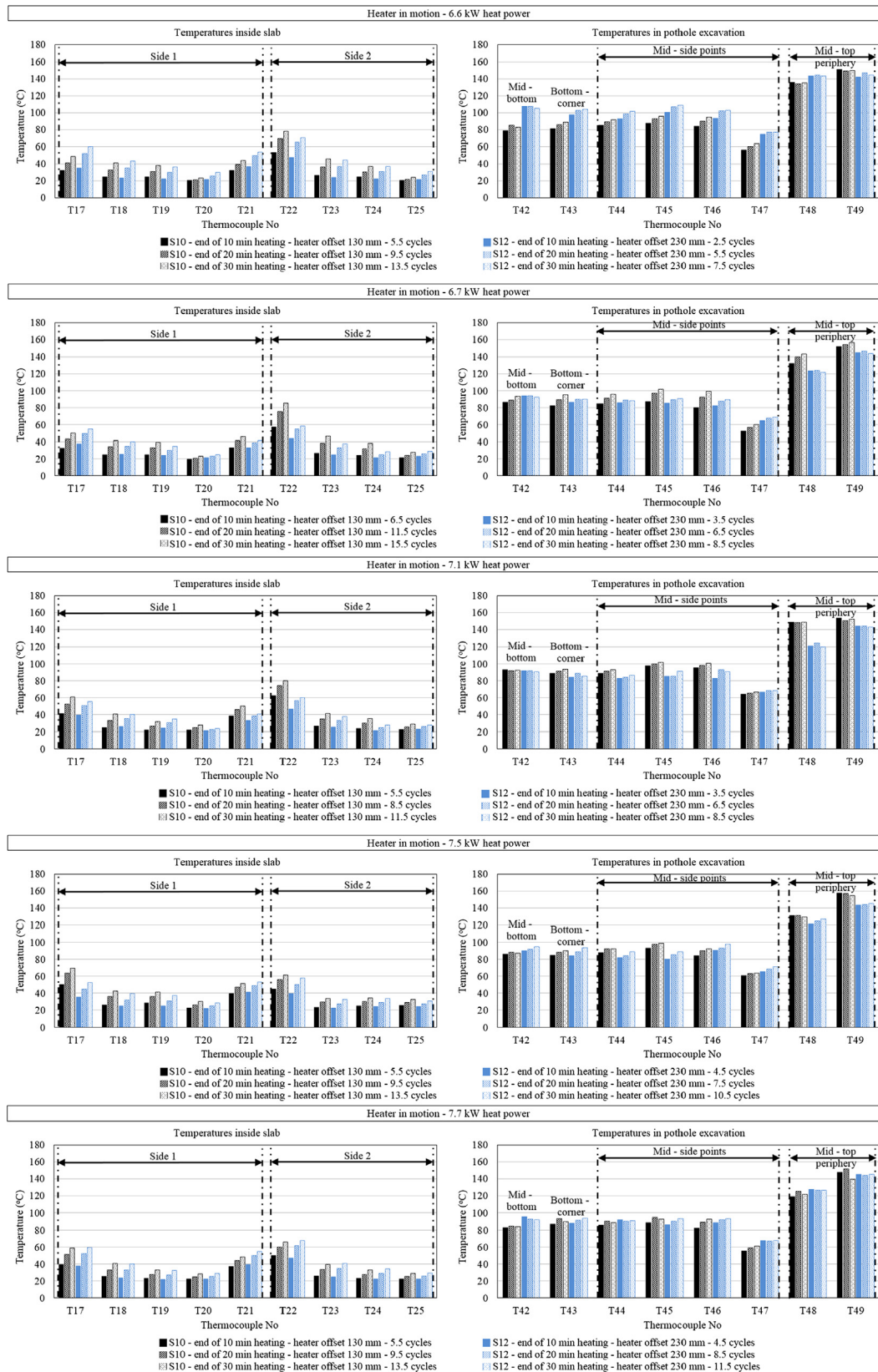


Fig. 12. Temperature distribution in 100 mm deep pothole excavation and moving heater.

excavation. For 230 mm offset, the temperature profile inside the slab did not change significantly. Specifically, T8 captured temperatures between 50 °C and 90 °C and temperatures for T9–T11 and

T14–T16 ranged from 25 °C to 75 °C and 20 °C to 55 °C respectively. T12 measured temperatures between 40 °C and 75 °C. T13 showed temperatures between 50 °C and 110 °C (Figs. 9 and 10).

5.2.3. Slabs with 100 mm deep pothole excavation

The heating effects of dynamic heating are shown in Figs. 11 and 12. Higher temperatures were seen between the excavation and inside the slab. Temperatures inside the slab were higher in the upper part of the slab and lower near the bottom of the slab.

Both temperature trends were seen for the 45 mm and 75 mm deep excavations. However, temperatures measured in the 100 mm deep excavation were even more uniform than the 45 mm and 75 mm deep excavations. Overall, temperatures for thermocouples T42 to T46 located within the excavation ranged

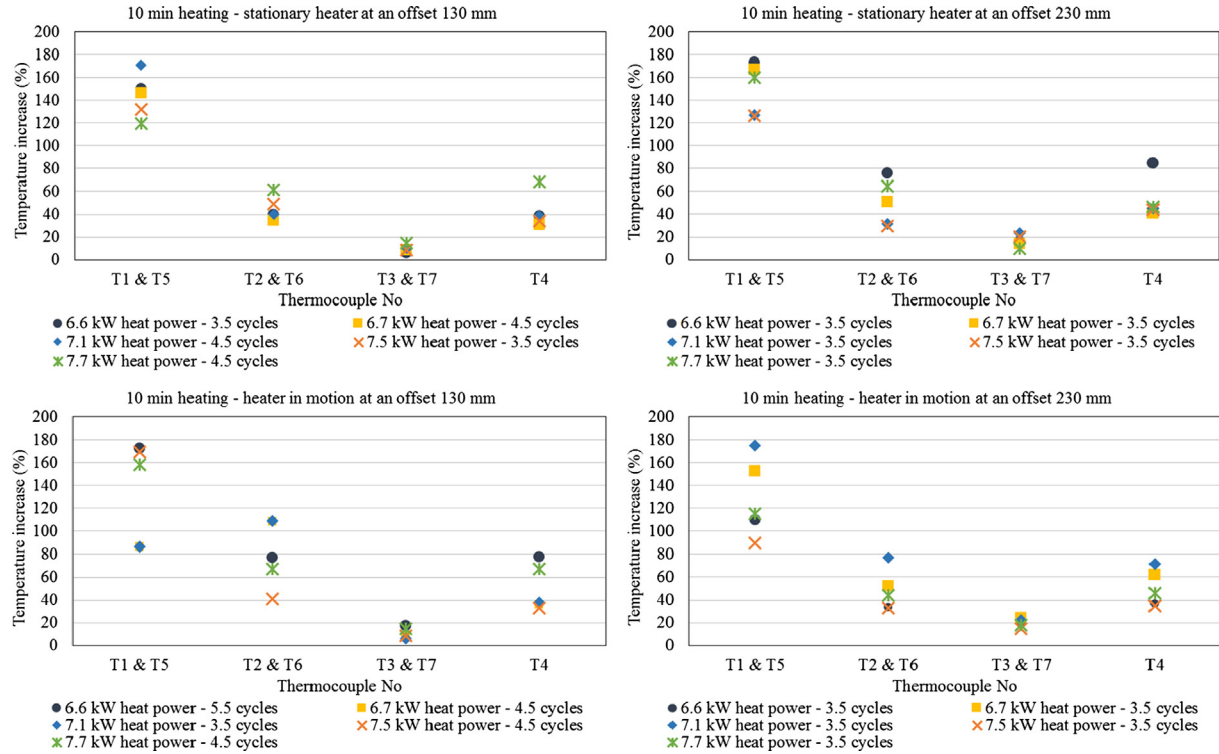


Fig. 13. Temperature increase percentage per thermocouple for approximately 10 min heating in 45 mm deep pothole excavation.

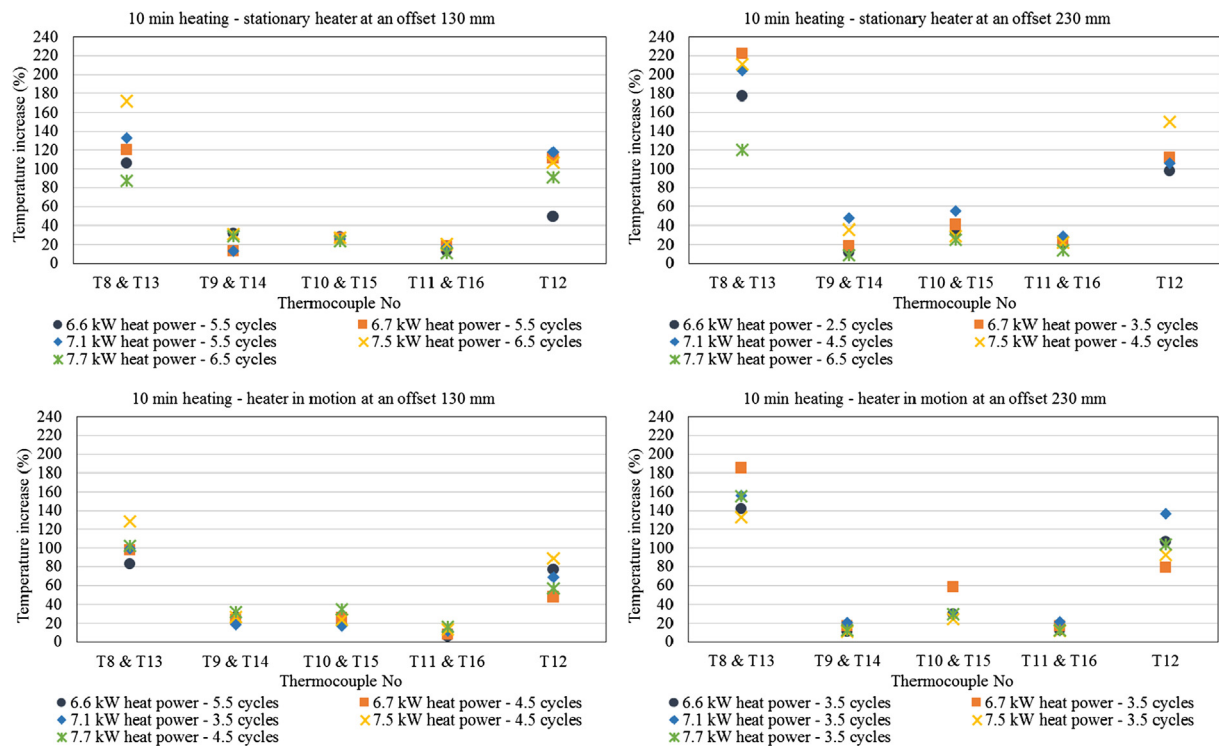


Fig. 14. Temperature increase percentage per thermocouple for approximately 10 min heating in 75 mm deep pothole excavation.

between 80 °C and 110 °C. The lowest temperatures in the excavation were seen for T47. For this sensor, for stationary and heater in motion at 130 mm offset, temperatures were between 50 °C and 65 °C. For 230 mm offset, temperatures ranged between 65 °C and 85 °C. The highest temperatures were observed in the top of

the excavation. These temperatures were captured by T48 and T49 and ranged between 110 °C and 160 °C. The effect of cooling at T48 due to heater moving across the excavation was mainly observed at heater operating heat powers between 6.7 kW and 7.7 kW.

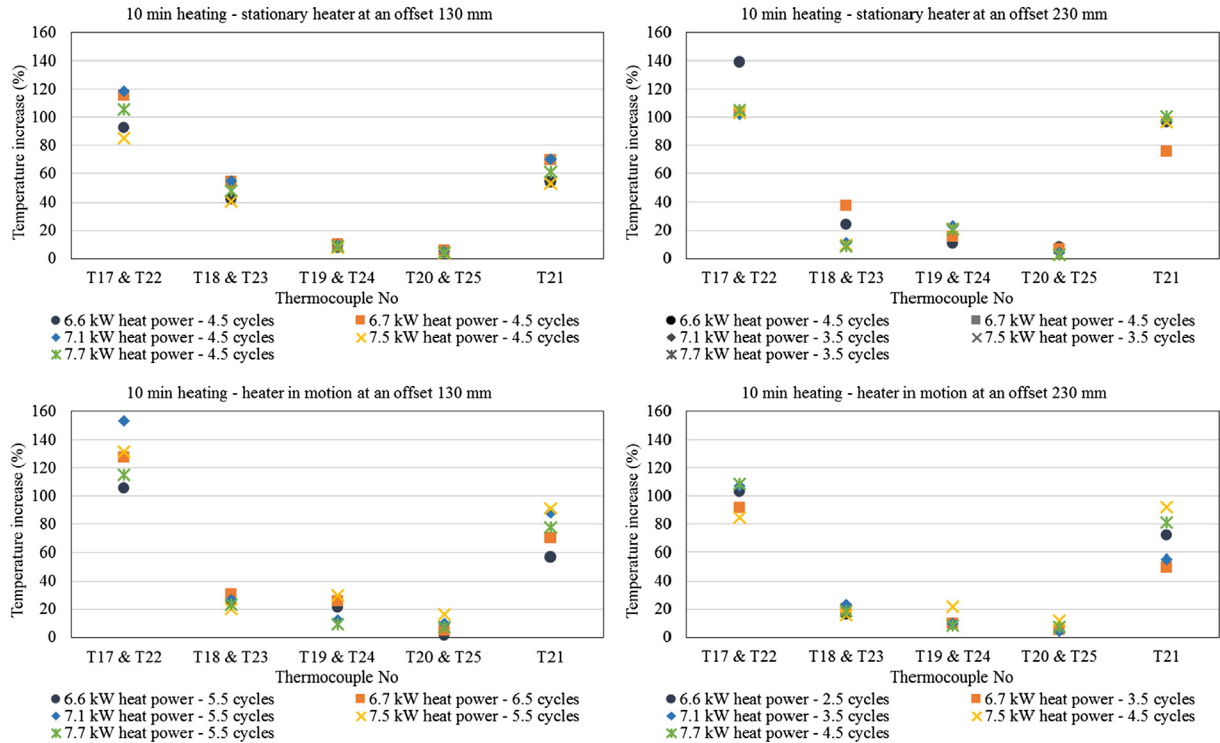


Fig. 15. Temperature increase percentage per thermocouple for approximately 10 min heating in 100 mm deep pothole excavation.

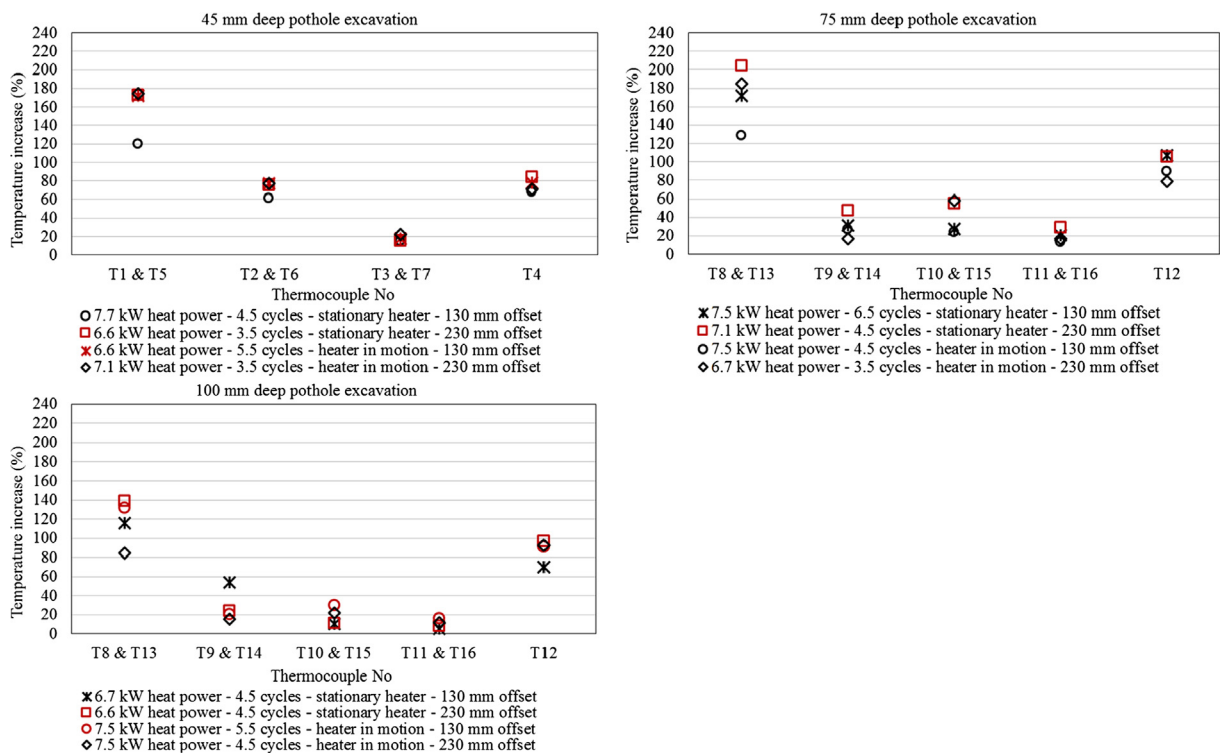


Fig. 16. Optimum dynamic heating methods for 45 mm, 75 mm and 100 mm deep pothole excavations.

Inside the slab mixture, the temperature for points closer to the top surface of the slab ranged from 30 °C to 70 °C (T17) and from 45 °C to 85 °C (T22). At lower depths, temperatures were between 20 °C and 55 °C. These temperatures were measured by T18–T20 and T23–T25 and were affected by the thermal properties of the mixture as already discussed. Finally, temperatures between 30 °C and 55 °C were captured from thermocouple T21 located below the bottom surface of the pothole excavation.

5.2.4. Optimum dynamic heating methods for 45 mm, 75 mm and 100 mm deep pothole excavations

For each temperature sampling point, the effect of heater power, offset and state above the excavations was analysed. This was discussed in Sections 5.2.1–5.2.3. The optimum heating method per pothole excavation was found by examining only the temperatures inside the slabs for approximately 10 min of heating. This was done because the results showed that the temperature increase rate inside the slab was higher for the first 10 min of heating than between 10 min and 30 min of heating. The optimum methods were chosen after finding the method

that offered the highest increase of temperature per thermocouple; was performed with lower number of heating-cooling cycles; and low heat power was used for the heating part of the cycles. The temperatures in the pothole excavation were not considered because the results showed that same temperature levels were achieved with each heating-cooling cycle. However, more heating time was needed to warm up the internal mixture of the slabs.

Initially, five best heating methods were chosen among the twenty thermal tests conducted per pothole excavation. Figs. 13, 14 and 15 present the concluded five methods. In these figures, the temperature increase per thermocouple location is compared against each method. Then, the optimum pre-heating method for 45 mm, 75 mm and 100 mm deep excavation was concluded and shown in Fig. 16, after eliminating the heating methods that did not meet the criteria discussed in the previous paragraph.

The time frame of heating-cooling cycles for optimum dynamic heating methods for all excavations are presented in Fig. 17. For 45 mm and 100 mm deep pothole excavations optimum heating methods with stationary and heater in motion are suggested. How-

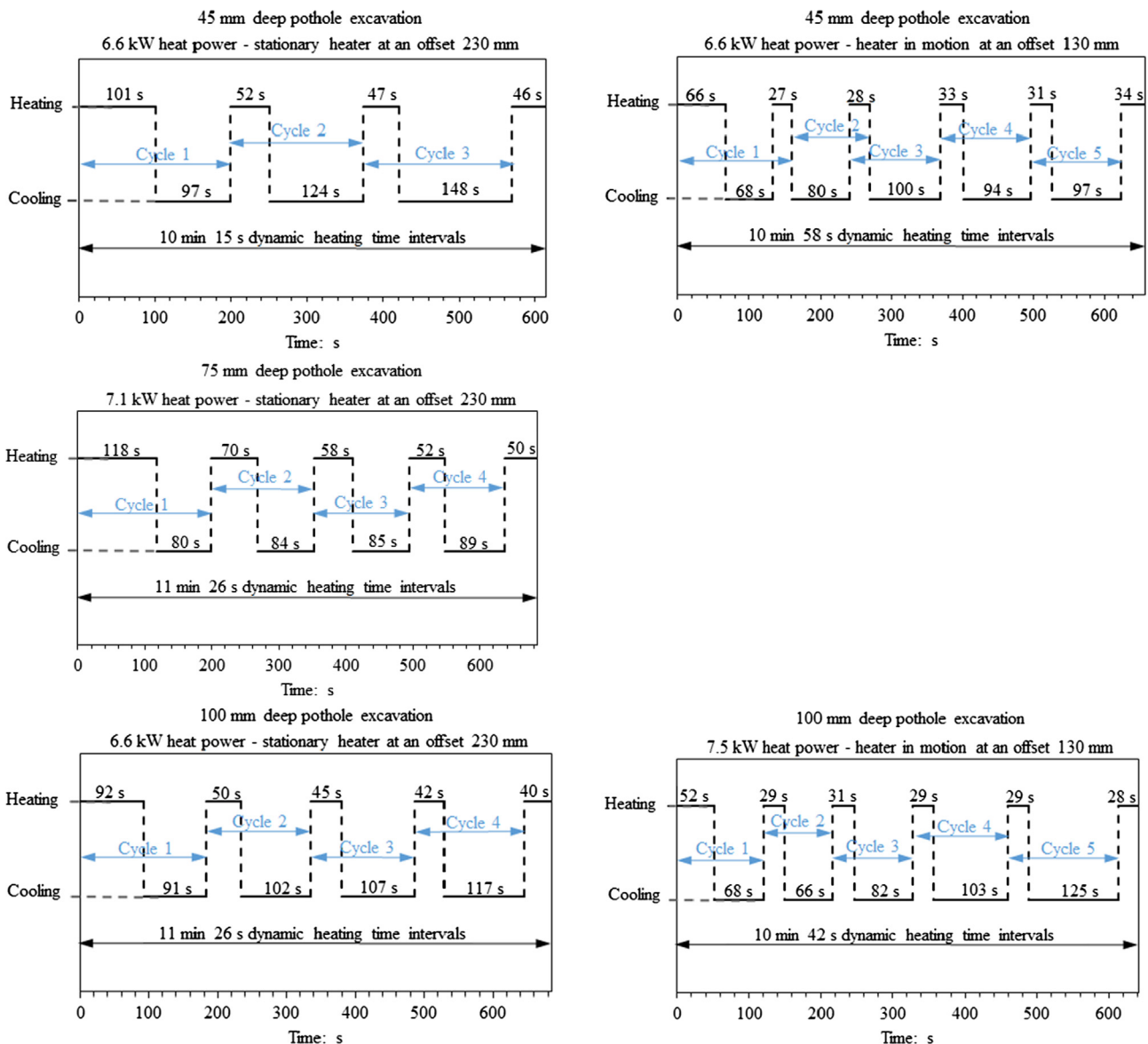


Fig. 17. Heating – cooling cycle times for optimum dynamic heating methods for 45 mm, 75 mm and 100 mm deep pothole excavations.

ever, to avoid overheating a larger area around a pothole excavation of $305 \times 165 \text{ mm}^2$, stationary heater is preferable.

6. Conclusions and future work

This study experimentally investigated the temperature profile in asphalt slabs and various depths of pothole excavations during dynamic infrared heat application. Temperatures were studied for various slab-heater configurations. These were 130 mm and 230 mm heater offsets and operating heat powers from 6.6 kW to 7.7 kW for stationary and moving heater. For each temperature sampling point, the effect of heater power, offset and state above the excavations was analysed. The main conclusions drawn from the research are the following:

- Temperatures under dynamic infrared heating in 45 mm, 75 mm and 100 mm deep pothole excavations and their host pavement were non – uniformly distributed.
- There was higher concentration of temperatures in the pothole excavation than inside the host pavement. This happened because temperatures in the excavations increase due to radiation. Whereas, the temperature profile inside the host pavement depends on the thermal properties of the asphalt mixture.
- Temperatures inside the host pavement increased more for the first 10 min of heating than for heating between 10 min and 30 min.
- Dynamically heating a pothole excavation ensures heating up of its external surfaces and internal asphalt mixture of host pavement without burning or overheating the asphalt. For this reason and to keep patching time to a minimum, 10 min–12 min dynamic heating time is better.
- It is suggested that 45 mm deep pothole excavation is dynamically heated for approximately 10 min with (a) 6.6 kW heat power and stationary heater above the pothole excavation at an offset from the asphalt surface 230 mm and (b) 7.5 kW heat power and heater in motion at an offset 130 mm. Method (b) preferred for pothole areas bigger than $305 \times 165 \text{ mm}^2$.
- It is suggested that 75 mm deep pothole excavation is dynamically heated for approximately 10 min with 7.1 kW heat power at an offset 230 mm.
- It is suggested that 100 mm deep pothole excavation is dynamically heated for approximately 10 min with (a) 6.6 kW heat power and stationary heater at an offset 230 mm and (b) 7.5 kW heat power and heater in motion at an offset 130 mm. Method (b) preferred for pothole areas bigger than $305 \times 165 \text{ mm}^2$.
- Dynamically heating the pothole excavation is intended to improve interface pothole repair bonding and therefore repair durability over time. The suggested optimum heating may be implemented in asphalt patch repairs prior to any pothole filling and compaction and after the failed asphalt is removed and the cavity is cleaned from debris and water.
- Further investigation is underway to evaluate interfacial bonding and long-term performance under moving wheel load as a quality improvement tests. In addition, the impact of preheating at different environment condition, host asphalt pavement mixtures and pothole fill materials are also under investigation.
- From the research it has also been concluded that future research must explore the effect of dynamic infrared heating in bitumen loses and disturbance of air voids in host pavement.
- The effect of thermal properties, asphalt absorptivity and surface roughness in infrared heated repairs should also be further investigated.

Conflict of interest

None.

Acknowledgement

This work was financially supported by International Chem-Crete Corporation, Texas, USA, EPSRC, Epicuro Ltd and DAC Consulting (UK) Ltd., Nynas UK AB and Conexpo (NI) Ltd supported by providing materials. Thermtest company supported in thermal conductivity instrument testing. Laboratory work was supported by Brunel University technical staff Neil Macfadyen and undergraduate student Kamal Ahmad.

References

- [1] A. Dawson, *Water in road structures: movement, drainage & effects*, Springer Science & Business Media, Dordrecht, the Netherlands, 2008.
- [2] R.S. McDaniel, J. Olek, A. Behnood, B. Magee, R. Pollock, *Pavement Patching Practices* (Project 20–05, Topic 44–04), National Cooperative Highway Research Program, Transportation Research Board, Washington, D.C., 2014.
- [3] J.R. Blaha, *Fabrication and Testing of Automated Pothole Patching Machine* (No. SHRP-H-674), Washington, D.C. Strategic Highway Research Program, National Research Council, 1993.
- [4] D.A. Anderson, H.R. Thomas, *Pothole Repair in Pennsylvania*. <https://docs.lib.purdue.edu/cgi/viewcontent.cgi?referer=&httpsredir=1&article=3367&context=roadschool&sei-redir=1&referer=http%3A%2F%2Fenr.com%2Fsearch%3Fq%3DPothole%2BRepair%2Bin%2BPennsylvania&go%3D%25E6%258F%2590%25E4%25BA%25A4&q%3Dn&form%3DQBLH&p%3Dupper%2Bgreat%2B>, 1984 (accessed 20 June 2018).
- [5] T.R. Clyne, E.N. Johnson, B.J. Worel, *Use of taconite aggregates in pavement applications* (No. MN/RC-2010-24), Minnesota Department of Transportation, Saint Paul, MN, USA, 2010.
- [6] L. Uzarowski, V. Henderson, M. Henderson, B. Kiesswetter, *Innovative Infrared Crack Repair Method*, in: *Proceedings of Congress et Exhibition de l'Association des Transports du Canada, 2011 Les Succes en Transports: Une Tremplin vers l'Avenir*, Edmonton, Canada, 2011.
- [7] T.J. Freeman, J.A. Epps, *HeatWurx Patching at Two Locations in San Antonio* (No. FHWA/TX-12/5-9043-01-1), Texas Transportation Institute, FHWA, Texas Department of Transportation, Austin, 2012.
- [8] C.W. Leininger, *Optimization of the infrared asphalt repair process*, Master's Thesis, University of Maryland. <https://search.proquest.com/openview/5d63e8ff20aa8561ec9f4e81b6fc75fe/1?pq-origsite=gscholar&cbl=187508&diss=y>, 2015 (accessed 20 June 2018).
- [9] H. Obaidi, B. Gomez-Mejide, A. Garcia, *A fast pothole repair method using asphalt tiles and induction heating*, *Constr. Build. Mater.* 131 (2017) 592–599, <https://doi.org/10.1016/j.conbuildmat.2016.11.0999>.
- [10] M.F. Modest, *Radiative heat transfer*, fourth ed., Academic press, Oxford, Amsterdam, 2013.
- [11] T.L. Bergman, F.P. Incropera, D.P. DeWitt, A.S. Lavine, *Fundamentals of heat and mass transfer*, seventh ed., John Wiley & Sons, Hoboken, New Jersey, 2011.
- [12] O.B. Andersland, B. Ladanyi, *Frozen ground engineering*, second ed., John Wiley & Sons Inc, Hoboken, New Jersey, 2004.
- [13] R. Mirzanamadi, P. Johansson, S.A. Grammatikos, *Thermal properties of asphalt concrete: a numerical and experimental study*, *Constr. Build. Mater.* 158 (2018) 774–785, <https://doi.org/10.1016/j.conbuildmat.2017.10.068>.
- [14] A. Hassn, M. Aboufoul, Y. Wu, A. Dawson, A. Garcia, *Effect of air voids content on thermal properties of asphalt mixtures*, *Constr. Build. Mater.* 115 (2016) 327–335, <https://doi.org/10.1016/j.conbuildmat.2016.03.106>.
- [15] B.A. Chadbourn, J.A. Luoma, D.E. Newcomb, V.R. Voller, *Consideration of hot mix asphalt thermal properties during compaction*, in: *Anonymous Quality management of hot mix asphalt*, ASTM International, 1996.
- [16] BS EN 13108 Part 1, *Bituminous mixtures – Material specifications*, British Standard Institute (BSI), 2016.
- [17] *Manual of contract documents for Highway works, Volume 1, Specification for highway works, Series 900 Road pavements – Bituminous bound materials*, 2008.
- [18] BS EN 12697 Part 35, *Bituminous mixtures – Test methods, Laboratory mixing*, British Standard Institute (BSI), 2016.
- [19] J.S. Miller, W.Y. Bellinger, *Distress identification manual for the long-term pavement performance program* (No. FHWA-HRT-13-092), United States, Federal Highway Administration, Office of Infrastructure Research and Development (2014).
- [20] Department of Transportation, *Standard Code of Practice, New Roads and Street Works Act 1991, Specification for the Reinstatement of Openings in Highways*, third ed. (England), Department of Transportation, 2010.
- [21] Omega, *Hermetically Sealed Thermocouple*. <http://www.omega.co.uk/pptst/HSTC.html>, 2016 (accessed: 14 May 2016).

- [22] J. Byzyka, D.A. Chamberlain, M. Rahman, Development of advanced temperature distribution model in hot-mix asphalt patch repair, in: Proceedings of the Institution of Civil Engineers – Transport. (2017) 1–11. <https://doi.org/10.1680/jtran.17.00022>.
- [23] M.D. Nazzari, S. Kim, A.R. Abbas, Evaluation of winter pothole patching methods, Columbus: FHWA, Ohio Department of Transportation, Publication FHWA/OH-2014/2, 2014.
- [24] K. Huang, T. Xu, G. Li, R. Jiang, Heating effects of asphalt pavement during hot in-place recycling using DEM, Constr. Build. Mater. 115 (2016) 62–69, <https://doi.org/10.1016/j.conbuildmat.2016.04.033>.
- [25] T. Mill, D.S. Tse, B. Loo, C.C.D. Yao, E. Canavesi, Oxidation pathways for asphalt, Prepr. ACS Div. Fuel Chem. (1992) 37–43.
- [26] Thermtest, Thermtest TLS-100, Portable transient line source, thermal conductivity meter for soil thermal conductivity testing as well as rock, concrete, and polymers. <https://thermtest.com/tls-100>, 2018 (accessed: 5 July 2018).
- [27] ASTM D5334, Standard Test Method for Determination of Thermal Conductivity of Soil and Soft Rock by Thermal Needle Probe Procedure, American Society for Testing and Materials (ASTM) (2000).
- [28] C.S. Blázquez, A.F. Martín, P.C. García, D. González-Aguilera, Thermal conductivity characterization of three geological formations by the implementation of geophysical methods, Geothermics 72 (2018) 101–111, <https://doi.org/10.1016/j.geothermics.2017.11.003>.
- [29] Y. Lu, W. Yu, D. Hu, W. Liu, Experimental study on the thermal conductivity of aeolian sand from the Tibetan Plateau, Cold Reg. Sci. Technol. 146 (2018) 1–8, <https://doi.org/10.1016/j.coldregions.2017.11.006>.
- [30] Overlockers, Alumina thermal paste (14g). <https://www.overclockers.co.uk/arctic-silver-alumina-thermal-paste-14g-th-006-ac.html>, 2018 (accessed 5 July 2018).
- [31] AASHTO, T166, Bulk specific gravity of compacted asphalt mixtures using saturated surface – dry specimens, American Association of State Highway and Transportation Officials (AASHTO) (2007).
- [32] F.L. Roberts, P.S. Kandhal, E.R. Brown, D. Lee, T.W. Kennedy, Hot Mix Asphalt Materials, Mixture Design and Construction, second ed., National Asphalt Pavement Association Education Foundation, Lanham, Maryland, 1991.
- [33] J. Norambuena-Contreras, A. Garcia, Self-healing of asphalt mixture by microwave and induction heating, Mater. Design 106 (2016) 404–414, <https://doi.org/10.1016/j.matdes.2016.05.095>.
- [34] L. Eppelbaum, I. Kutasov, A. Pilchin, Methods of Thermal Field Measurements. In: Applied Geothermics, Lecture Notes in Earth System Sciences, Springer, Berlin, Heidelberg, 2014, pp. 151–159. https://doi.org/10.1007/978-3-642-34023-9_3.
- [35] P. Pan, S. Wu, X. Hu, P. Wang, Q. Liu, Effect of freezing-thawing and ageing on thermal characteristics and mechanical properties of conductive asphalt concrete, Constr. Build. Mater. 140 (2017) 239–247, <https://doi.org/10.1016/j.conbuildmat.2017.02.135>.
- [36] P. Pan, S. Wu, Y. Xiao, P. Wang, X. Liu, Influence of graphite on the thermal characteristics and anti-ageing properties of asphalt binder, Constr. Build. Mater. 68 (2014) 220–226, <https://doi.org/10.1016/j.conbuildmat.2014.06.069>.
- [37] G. Kyriakidis, M. Santamouris, Using reflective pavements to mitigate urban heat island in warm climates—results from a large scale urban mitigation project, Urban Clim. 24 (2018) 326–339, <https://doi.org/10.1016/j.uclim.2017.02.002>.
- [38] R.B. Stephens, G.D. Cody, Optical reflectance and transmission of a textured surface, Thin Solid Films 45 (1977) 19–29.